Resources Policy 58 (2018) 90–96

Contents lists available at ScienceDirect

Resources Policy

journal homepage: www.elsevier.com/locate/resourpol

Analysis of life-cycle GHG emissions for iron ore mining and processing in China—Uncertainty and trends

Yu Gan*, W. Michael Griffin

Engineering and Public Policy, Carnegie Mellon University, 5000 Forbes Avenue, Pittsburgh, PA, USA

ABSTRACT

Total iron ore demand in China grew to 1.1 billion tonnes in 2013 as a result of ongoing urbanization and massive infrastructure development. Iron ore and steel production are major sources for greenhouse gas (GHG) emissions. Since China has committed to lowering carbon intensity to meet climate change mitigation goals, detailed studies of the energy use and GHG emissions associated with iron ore mining and processing can aid in quantifying the impact and effectiveness of emissions reduction strategies. In this study, a life-cycle model for mining and processing of Chinese iron ores is developed and used to estimate GHG emissions. Results show that the mean life-cycle GHG emissions for Chinese iron ore production are 270 kg CO_2e/tonne, with a 90% confidence interval ranging from 210 to 380 kg CO_2e/tonne. The two largest contributors to overall GHG emissions are agglomeration (60%) and ore processing (23%). Iron content (ore grade) varies from 15% to 60% and is the largest contributor (40%) to the uncertainty of the results. Iron ore demand growth and the depletion of rich ore deposits will result in increased exploitation of lower grade ores with the concomitant increase in energy consumption and GHG emissions.

1. Introduction

China's urbanization and its associated massive infrastructure development are creating rising demand for iron ore and steel production (Shen et al., 2005). Total iron ore demand grew from 200 million tonnes in 2001 to 1.1 billion tonnes in 2013. With all grades converted to 62% Fe iron content, the rise in ore use is equivalent to an average yearly increase of 15% (China Steel Yearbook, 2014). China is the world's largest iron ore producer and consumer, responsible for 45% of total global production and 55% of total consumption (U.S. Geological Survey website). This consumptive growth leads to the depletion of iron-ore resources and increased exploitation of lower quality ores (China Steel Yearbook, 2014). Produced, crude ore grade has dropped from 30% Fe to 27% Fe between 2006 and 2012 (China Steel Yearbook, 2014). Processing lower grade ores for an equivalent mass of ore concentrate requires higher energy intensity, potentially resulting in increased GHG emissions (Norgate and Haque, 2010).

As the largest GHG emitter (Friedlingstein et al., 2014), China committed to lowering the carbon intensity of its economy by 60% to 65% from the 2005 level by 2030 (Karali et al., 2014). To meet this commitment, China needs to develop a multitude of GHG emissions reduction strategies. The iron and steel sector could be a major focus, as it contributes about 12% of the country's total GHG.

In addition to direct GHG emissions within the iron ore sector, iron ore production can lead to indirect emissions from other sectors that supply required goods and services, such as raw material, energy production, and transportation. This study uses life-cycle assessment (LCA), which traces the product impacts under study (in this case, iron ore), and includes impacts from relevant upstream and downstream processes (cradle to gate). LCA is a widely used method of researchers and policymakers for decision making (Scott Matthews et al., 2014).

Studies have determined China's iron and steel sector emissions using a variety of approaches (Karali et al., 2014; Li et al., 2016; Chen et al., 2014; Hasanbeigi et al., 2013), but these studies either did not model the upstream emissions for iron production and processing, as the objective of the work was to determine the size of the sectorial emissions or to explore mitigation possibilities. Li et al. did include upstream ore mining and processing but aggregated the results for coal and iron ore production (Li et al., 2002; Iosif et al., 2008). Stewart (2001) suggest mining data availability, data quality, and representativeness as the primary reasons there are few LCA studies for minerals mining in general.

Two LCA studies estimate the GHG emissions of iron ore mining and processing in Australia and Brazil (Norgate and Haque, 2010; Ferreira et al., 2015). Norgate and Haque estimated Australian iron ore mining and ore processing GHG emissions at 12 kg CO_2e/tonne (Norgate and

* Corresponding author.
E-mail address: gany@andrew.cmu.edu (Y. Gan).

https://doi.org/10.1016/j.resourpol.2018.03.015
Received 22 November 2017; Received in revised form 26 February 2018; Accepted 26 March 2018
Available online 12 April 2018

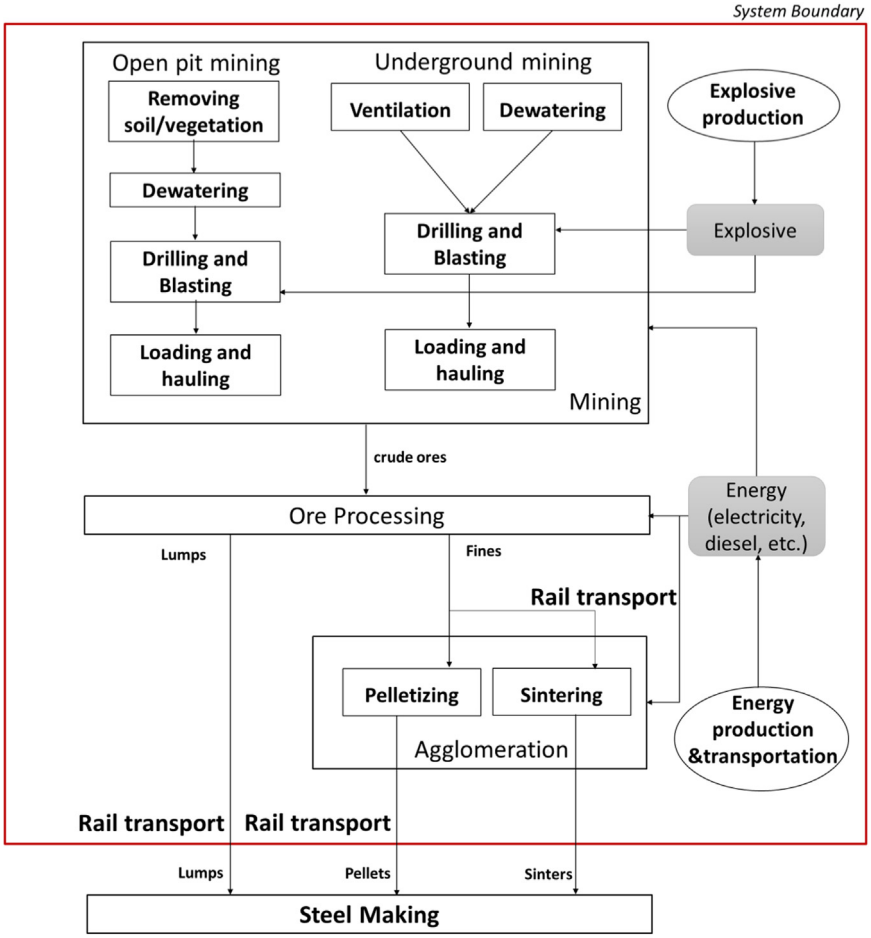

Fig. 1. Chinese iron ore mining flowsheet and the associated LCA system boundary. Rectangular boxes indicate unit operations of iron mining and processing; Shaded boxes indicate energy and explosives input; Rounded boxes indicate upstream processes of energy and explosives production.

Haque, 2010). Ferreira et al. (2015) reported Brazilian these emissions as 13 kg CO_2e/tonne. With general uncertainty related to data and LCA methods these results should be considered the same (Scott Matthews et al., 2014).

The GHG emissions estimates can slightly due to geological and operating conditions (Ferreira et al., 2015) and there are substantial differences in Chinese ore mining compared to these studies, such as greater average mine depth and lower grade ore extraction. These attributes are expected to change the China's emissions estimate (China Steel Yearbook, 2014).

This study develops a life-cycle model to determine the GHG emissions of iron ore mining and processing in China. By using data from varied sources and at different levels of aggregation, the study provides average sectoral estimates, and uncertainty ranges for the life-cycle inventory (LCI) results. Sensitivity analysis is used to determine the parameters that drive model results and highlight future data needs and areas requiring further study. Based on the results, the study further discusses viable ways of GHG emissions reduction and provide utility for policy makers.

2. Methods

The following presents data and methods used for estimating GHG emissions from Chinese iron ore production. The emissions embodied in three forms of iron products (lumps, sinters, and pellets; defined below) are analyzed. This analysis includes GHG emissions throughout the mining and ore processing stages, as well as indirect emissions associated with the consumption of energy and explosives during the mining and concentrating processes.

2.1. Goal, scope, system boundary, and functional unit

The goal of the study is to determine the GHG emissions of Chinese iron ore mining. The iron ore production system and the system boundary used are shown in Fig. 1 and include mining, ore processing, and agglomeration stages.

Open pit and underground mining are modeled. The functional unit is one metric ton of processed iron-ore delivered to the blast furnace, the entry point to the steel making process. The blast furnace requires ore with an Fe content of 60% or higher. Lumps, sinters or pellets are all used as feedstock. These three forms of iron ore are treated as equivalent in this study as they all are sized to between 10 and 30 mm, and have an iron content of 60% or higher.

The final results are presented in terms of 100-year global warming potentials (GWPs), using GWP factors reported by the Intergovernmental Panel on Climate Change (IPCC) assessment report (IPCC, 2007). Also, all results are presented as CO_2 equivalents (CO_2e) as some of the aggregated upstream emissions factors used are reported as CO_2e and include non-CO_2 emissions, e.g., methane and N_2O. This approach was made necessary as some data sources are aggregated making updating to more recent values impossible. However, as the majority of emissions in the system are CO_2, the differences should be small.

Fig. 1 shows the detailed mining steps for both open pit and underground mining. Crude ore is delivered by diesel truck to the processing facilities, i.e., “loading and hauling” as depicted. The ore is sized, and Fe content increased if needed. High-grade ore (> 60% Fe content) requires only simple crushing and screening. The generated

iron ore lumps are suitable for direct use in the blast furnaces and are shipped by rail to the steel mill. Low-grade ore (< 60% Fe content) undergoes multiple processing steps to increase the overall iron content. These include crushing, screening, milling, flotation or magnetic separation, followed by filtering and drying. These processes produce fines with an iron content greater than 60% and smaller than 0.1 mm.

After ore processing, fines require agglomeration, by sintering or pelleting, to form aggregates for use in the blast furnace. Pelletizing plants are usually located at or near the iron ore mines and assumed so located for this study. After pelleting, the pellets are transported to steel mills, where the blast furnaces are located. Sintering plants, co-located at the steel mills, receive fines for processing directly from the mines and transfer the sinters to the blast furnace (Kogel, 2006). All three ore forms ship to the steel mill by rail (China Steel Yearbook, 2014).

2.2. Estimation approaches

Three estimation approaches were applied to calculate GHG emissions using data with different aggregation levels and from a variety of sources.

2.3. Approach I (bottom-up modeling)

2.3.1. Mining

In this study, a bottom-up approach is used to estimate GHG emissions associated with each individual mining process of open pit mining. Open pit mining accounts for 87% of the Chinese iron ore extraction (China Steel Yearbook, 2014). Because of the lack of disaggregated data related to underground mining, the bottom-up assessment is applied only to open pit mining. Table 1 describes the assumptions and parameters used in the assessment. Detailed calculations and a discussion of the data and its representativeness are reported in the SI Section Approach I: bottom up model.

The bottom-up analysis of open pit mining includes the following stages:

2.3.2. Vegetation and soil removal

Vegetation and soil are removed to expose the ore seam. GHG emissions arise from microbial decomposition of the removed biomass and soil (soil organic carbon degradation). Additionally, a debt accrues due to reduced photosynthetic productivity during the life of the mine due to the removed biomass. The CO_2 emissions estimates account for changes in the soil carbon stock, vegetation carbon stock, net primary production of the mining area and ground disturbance area over the mine lifetime. Emissions associated with heavy truck and tractor diesel use from removal and transport of the soil and vegetation were estimated using bulldozer load factors, fuel consumption and estimated distances to dumping sites (Table 1).

2.3.3. Drilling and blasting

Greenhouse gas emissions can arise through diesel use from drilling blasting boreholes and production of the explosives used for blasting. The drilling diesel use for extracting one tonne of crude ore was calculated as unit diesel use for drilling one tonne of rocks adjusted using the stripping ratio, defined as the ratio of overburden to the extracted crude ores. The explosives used for blasting were adjusted in the same way and coupled with the explosives emissions factor (Table 1) to determine GHG emissions associated with explosive use. The emissions factor represents emissions from its production, transportation, and detonation.

2.3.4. Dewatering

Ground and rainwater accumulate continuously during mining and require removal. The electricity consumption for dewatering was calculated based on the water volume, pumping efficiency, and pumping water head.

2.3.5. Loading and hauling

After blasting, the ore is removed from the mine via truck and sent to the ore treatment processes. Emissions arise from loading ores on trucks and hauling ore to the processing plant and hauling waste rock to the disposal area. Diesel consumption is based on a tonne of crude ore produced. Conversion from this basis to the per tonne functional unit basis accounts for the Fe loss rate during processing of the original ore and the amount of ore needed to reach the final ore grade.

2.3.6. Ore processing

The Ferrous Metal Mining Statistical Yearbook of China provides data for 53 iron ore processing plants (Kogel, 2006). These facilities represent 18% of total iron ore production and 83% of pig iron production in China, respectively. The data included electricity use for one tonne of crude ore treatment, ore grade before and after processing and Fe loss rate. These data were used to estimate energy use and GHG emissions. The Akaike Information Criterion (AIC) method was used to determine the best-fit distributions for modeling parameters related to ore processing energy use. See the Ore Processing section of the SI for more detail.

2.3.7. Rail transportation

In addition to the data describe in the Ore Processing section, the statistical yearbook provides latitudes and longitudes for the ore processing facilities and 66 Chinese steel mills (Ferro Metallurgy and Mining Statistical Yearbook 2011, 2012). Assuming the steel mills acquire raw material from the nearest processing plant, the distance for the closest processing plants to a mill was identified using the great-circle distance calculated by Haversine's Formula (Robusto, 1957) and a circuity factor of 1.5 for rail (Akaike, 1974). The model uses a discrete distribution of 66 distances, weighted by the percentage of total pig iron production from each steel mill. Fuel consumption associated with rail transportation was calculated using the distance distribution and fuel consumption factor. The fuel consumption factor is based on public LCI databases and existing literature (Ferreira et al., 2015; SimaPro LCA software, 2008; Life Cycle Inventory Database, 2014). The Approach II and Approach III described below also use these data for rail transportation.

2.3.8. Agglomeration

Agglomeration takes iron fines, mixed with other materials (e.g., coke, limestone, etc.) and high temperatures, to form larger particles compatible with the blast furnace. The thermal process requires fuel for heating and is a major source for GHG emissions. About 75% of the Chinese iron ore fines are transported to steel mills for sintering, while the remaining is pelletized at the mining site (China Steel Yearbook, 2014). The GHG emissions associated with sintering were modeled using a uniform distribution ranging from 200 to 280 kg CO_2e/tonne iron fines (Iosif et al., 2008; Kumar and Srinivasan, 2010; World Steel Life Cycle Inventory, 2000). GHG emissions from pelletizing processes were modeled as a uniform distribution from 25 to 30 kg CO_2e/tonne iron fines (Iosif et al., 2008; Kumar and Srinivasan, 2010; World Steel Life Cycle Inventory, 2000). The emissions of the agglomeration stage were calculated as a weighted average of the pelletizing and sintering processes emissions (using the fraction of iron ore produced by the two agglomeration techniques).

2.3.9. Diesel and electricity emissions factors

Diesel and electricity use related GHG emissions associated calculations used emissions factors taken from the literature. Various studies estimate the emissions factor of diesel fuel and include the emissions from oil production, refining, transportation and combustion (Stewart, 2001; Ferreira et al., 2015; AusLCA datasets, 2011; Venkatesh et al., 2010; Lixue et al., 2013). Using these data sources, a uniform distribution of 90 to 100 gCO_2e/MJ was constructed. Detailed data and associated discussion of data applicability are presented in the

Table 1
Parameters used for bottom up modeling of open pit mining.

Processes	Details and assumptions	Emissions source	Parameter (units)	Value distributions (cardinal parameters)	Data sources
Vegetation and soil removal	Soil/vegetation carbon stock loss	Soil/vegetation carbon	Soil carbon stock (kg CO_2e/m^2) [a]	Uniform[b] (10, 33)	(Yu et al., 2007)
			Vegetation carbon stock (kg CO_2e/m^2)	Uniform (0, 24)	(Ruesch and Gibbs, 2008; Fang et al., 2007)
			Ground disturbance[c] (m^2/tonne)	Uniform (0.85, 1)	(China Steel Yearbook, 2014; Benxi Iron & Steel Group; Mines Overview; Anshan Iron and Steel, 2013; Chang, 2010)
			Mine lifetime (years)	Triangular[d] (2, 10, 30)	(China Steel Yearbook, 2014; Li et al., 2002; World Steel Life Cycle Inventory, 2000; Lixue et al., 2013; Anshan Iron and Steel, 2013; Chang, 2010)
	Loss of photosynthetic productivity during project life time	Net primary production (NPP)	NPP ($gC/m^2/yr$)	Uniform (0.34, 0.36)	(Haberl et al., 2007; Imhoff and Bounoua, 2006; Pidwirny)
	Vegetation and soil clearance with bulldozer CAT D11R[e]	Diesel fuel	Bulldozer load factor for soil clearance (%)[f]	Uniform (50,65)	(Kecojevic and Komljenovic, 2011)
		Diesel fuel	Bulldozer load factor for vegetation clearance (%)	Uniform (35,50)	(Kecojevic and Komljenovic, 2011)
	Heavy trucks for soil transport	Diesel fuel	Distance of dumping soil (km)	Uniform (5,10)	(China Steel Yearbook, 2014; World Steel Life Cycle Inventory, 2000; Lixue et al., 2013; Anshan Iron and Steel, 2013; Chang, 2010; Tannant and Regensburg, 2001)
			Fuel consumption factor (MJ/tonne.km)	Uniform (1.0,1.5)	(Stewart, 2001; Ferreira et al., 2015; Tannant and Regensburg, 2001)
Drilling	Electric-diesel engine powered rotary drills	Diesel fuel	Diesel use in drilling holes for blasting out one tonne of rocks (MJ/tonne)	Uniform (0.3,1.0)	(China Steel Yearbook, 2014; Norgate and Haque, 2010; World Steel Life Cycle Inventory, 2000; Lixue et al., 2013; Anshan Iron and Steel, 2013; Chang, 2010; Teale, 1965)
			Stripping ratio (tonne of waste rock/tonne of iron ore) [g]	Triangular (2, 3, 5)	(China Steel Yearbook, 2014; World Steel Life Cycle Inventory, 2000; Lixue et al., 2013; Anshan Iron and Steel, 2013; Chang, 2010)
Blasting	Ammonium nitrate/fuel oil mixture explosive for blasting	Explosives	Explosive for blasting one tonne of rocks (kg/tonne)	Triangular (0.07, 0.14, 0.2)	(China Steel Yearbook, 2014; Norgate and Haque, 2010; World Steel Life Cycle Inventory, 2000; Lixue et al., 2013; Anshan Iron and Steel, 2013; Chang, 2010; Teale, 1965; New Millennium Capital Corp, 2010)
Dewatering	Pumping water from groundwater intrusion	Electricity	Ratio of water and mining ores (m^3/tonne)	Triangular (0, 0.4, 4)	(China Steel Yearbook, 2014; World Steel Life Cycle Inventory, 2000; Lixue et al., 2013; Anshan Iron and Steel, 2013; Chang, 2010; Domingues et al., 2013)
			Pumping efficiency (%)	Uniform (50, 85)	(Domingues et al., 2013; Jones et al., 2006; Volk, 2013)
			Pumping water head (m)	Uniform (100, 300)	(China Steel Yearbook, 2014; World Steel Life Cycle Inventory, 2000; Lixue et al., 2013; Anshan Iron and Steel, 2013; Chang, 2010)
Ore Loading	Front-end loader	Diesel	Diesel use for loading one tonne of rocks (MJ/tonne)	Triangular (2.5, 8.5, 18.5)	(Volk, 2013; Pero, 2011)
Ore Hauling	Ore carriers (heavy trucks)	Diesel	Diesel use for hauling per unit (MJ/tonne.km)	Uniform (1.5, 4.8)	(Kecojevic and Komljenovic, 2011; Volk, 2013; Analysis of Diesel Use for Mine Haul and Transport Operations, 2010)
			Hauling distance (km)	Triangular (2, 4.5, 6)	(China Steel Yearbook, 2014; World Steel Life Cycle Inventory, 2000; Lixue et al., 2013; Anshan Iron and Steel, 2013; Chang, 2010; Tannant and Regensburg, 2001)

[a] Carbon stock in top 1 m soil is calculated. Soil carbon stock and vegetation carbon stock are correlated with net primary production, detail in SI.
[b] Uniform (x, y) means the value for the parameter in the model is a uniform distribution, with a lower bound of x, and a upper bound of y.
[c] Ground disturbance is the quotient of the mining area and the annual iron ore production, in unit of m^2/tonne.
[d] Triangular (a, b, c) means the value for the parameter in the model is a triangular distribution, with a lower bound of a, a upper bound of c, and most likely value of b.
[e] Caterpillar D11R is a type of large bulldozer, mainly used in mining industry for push-loading scrapers.
[f] Bulldozer load factor is the percentage of bulldozer working load compared with the full capacity.
[g] The parameter of stripping ratio is also used in modeling the processes of blasting, loading and hauling, but is not listed repeatedly in the table.

Supporting Information (SI) section - Emissions factor of diesel fuel.

Electricity was assumed to be the Chinese grid mix estimated and modeled as a uniform distribution from 760 to 830 gCO_2e/kWh for different regions (China's Regional Grid Baseline Emission Factors, 2010). The 10% range is small compared to the range of emissions factors from 260 to 810 g CO_2e/kWh reported for the different regions in the U.S (Emissions & Generation Resource Integrated Database). Thus, the estimate used here might lead to an underestimation of the actual uncertainty. The SI section on Emissions factor for grid mix electricity details the data and their applicability. Approach II and Approach III will also use the estimates listed here for diesel and electricity emissions factors.

2.4. Approach II: estimation based on aggregate mining level observations

This approach uses data for electricity use, diesel use, stripping ratio and explosive use for extracting per ton of rocks from 55 Chinese mines (24 underground and 31 open pit) published by the Chinese government's Department of Metallurgy to estimate the energy use of iron ore mining (Ferro Metallurgy and Mining Statistical Yearbook 2011, 2012). As above, the AIC method was used to develop the most likely probability distribution for the aggregated data for each parameter for each category of mine (open pit and underground). The parameters were then used to estimate the energy use and associated GHG emissions of underground and open pit mining. Table A6 in SI shows the parameters and their fitted probability distributions. Approach II used the same methods and data sources as Approach I to estimate the emissions associated with ore processing, rail transportation and agglomeration.

2.5. Approach III

Aggregated energy for the iron ore mining and processing stages is derived from The Chinese Energy Statistics Year Book (2012). The total energy consumption results from consumption of 1.8 kg of coal, 1.2 kg of coke, 25 MJ of diesel fuel and 34 kWh electricity use to produce a tonne of iron ore in 2013. The GHG emissions energy emission factors for the different energy sources are listed in SI section Approach III.

2.6. Monte Carlo simulation

Monte Carlo simulation was used to generate the probability distribution of the life cycle GHG emissions for each approach and to understand parameter uncertainty associated with each estimate. Spearman's rank correlation coefficient for each parameter was calculated to determine that parameter's corresponding influence on the variance of the final result (Ferson, 1996). The study used Palisade's @ Risk™ software for Monte Carlo simulation and sensitivity analysis.

3. Results and discussion

This study developed multiple estimates for the GHG emissions from iron ore mining and processing in China. Using data at different levels of aggregation three approaches were applied to calculate GHG emissions for different mining and ore processing scenarios. Fig. 2 shows multiple GHG emissions estimates for the mining phase of the analysis. The bottom up (Approach I) provided an estimate for open pit mining. Approach II used more aggregate government sourced data, and estimated emissions for both open pit (surface mining) and underground mining (shaft mining), as well as a combined value based on the weighted average of the two mining processes. Approaches I and II result in mean emissions estimates for open pit mining of 39 and 35 kg CO_2e/tonne of ore, respectively. The two estimates vary by approximately 10%.

The bottom up approach (Approach I in Fig. 2) yielded GHG emissions estimates for each individual mining process. The largest GHG emissions source for open pit mining was iron ore loading and hauling (67% in total mining emissions), where diesel powered loaders and trucks are used to move ore from mine for further processing. The second largest contributor is related to vegetation and soil removal, which includes GHG emissions from microbial decomposition of the removed biomass and soil and lost photosynthetic productivity during the life of the mine. These GHG emissions account for 24% in total mining emissions and are neglected in prior studies (Norgate and Haque, 2010; Ferreira et al., 2015).

The mean emissions of underground mining are estimated as 34 kg CO_2 e/tonne of ore by Approach II. Using this estimation approach, the values for open pit and underground mining techniques are essentially the same. When the ore is near the surface, open pit mining should result in reduced energy-use and emissions as it avoids the energy used for ventilation. Ventilation accounts for more than 30% of total energy use in underground mining. However, many deposits in China are deeply buried (more than 200 m from the surface). The energy consumption for overburden removal thus offsets any potential energy savings from not requiring ventilation. Currently, open pit mining produces 87% of China's iron ore. However, many deposits in China are deeply buried (more than 200 m from the surface), and the energy consumption for overburden removal in open pit mining offsets the energy use in ventilation for underground mining. Although most of the iron ores (87%) in China are currently extracted through open pit mining, there is a trend toward greater use of underground mining techniques as shallow ore deposits are depleted (China Steel Yearbook, 2014).

The right panel of Fig. 2 shows the total iron ore life-cycle GHG emissions estimated by the three approaches. The mining stage uses the combined mining values shown in the left panel for “Mining, overall approach II.” The mean estimates for the totals shown in the right panel range from 270 to 280 kg CO_2e/tonne. The 4% difference between the estimates is within the uncertainty of LCA, in general, as LCA cannot model reliably differences this small (Scott Matthews et al., 2014).

The GHG emissions values include both direct emissions released during the mining and ore processing, and indirect emissions from upstream energy and explosive production and transportation. The direct GHG emissions are 200 kg CO_2e/tonne, accounting for about 70% of the life cycle emissions calculated with Approach I.

In the overall emissions values the agglomeration process is responsible for the majority of the GHG emissions arising from the process heat requirements. Sintering has significantly higher GHG emissions than pelletizing. The sintering emissions range from 200 to 280 kg CO_2e/tonne while pelletizing emissions are lower at 25 to 30 kg CO_2e/tonne. Thus, the fraction of sinters in the mixture feed to the steel mills blast furnace impacts the overall GHG emissions estimates for the agglomeration stage and the overall process.

Currently in China 70–80% of the blast furnace feed are sinters. If the current mix was replaced with 100% pellets, life-cycle GHG emissions would be 130 kg CO_2e/tonne iron ore, which is 140 kg CO_2e/tonne iron ore (52%) lower than current emissions calculated with Approach II. Increasing the fraction of pellets would significantly reduce GHG emissions, however, the additional investment would be required to develop techniques and to install new facilities that were adapted to the feedstock change. Additionally, the production cost of pelletizing is higher than sintering. In 2013, the market price of pellets was $15–40 per tonne higher than sinters (China Steel Yearbook, 2014). Thus, replacing sinters with pellets would reduce GHG emissions by 170 to 260 kg CO_2e/tonne but raise the iron ore feedstock cost for steel mill by $15–40 per tonne. The cost of GHG emissions mitigation is then estimated to be $60–240 per tonne of CO_2 equivalent.

The pelletizing technique was developing fast in China from 2001 to 2011. During the period, the annual pellets production increased from 18 million tonnes to 204 million tonnes, and the proportion of pellets in total iron ore feed to the blast furnace grew from 7% to 19%. However, the growth of pellet production has stagnated since 2012, and the proportion of pellets in total iron ore feed to the blast furnace declined

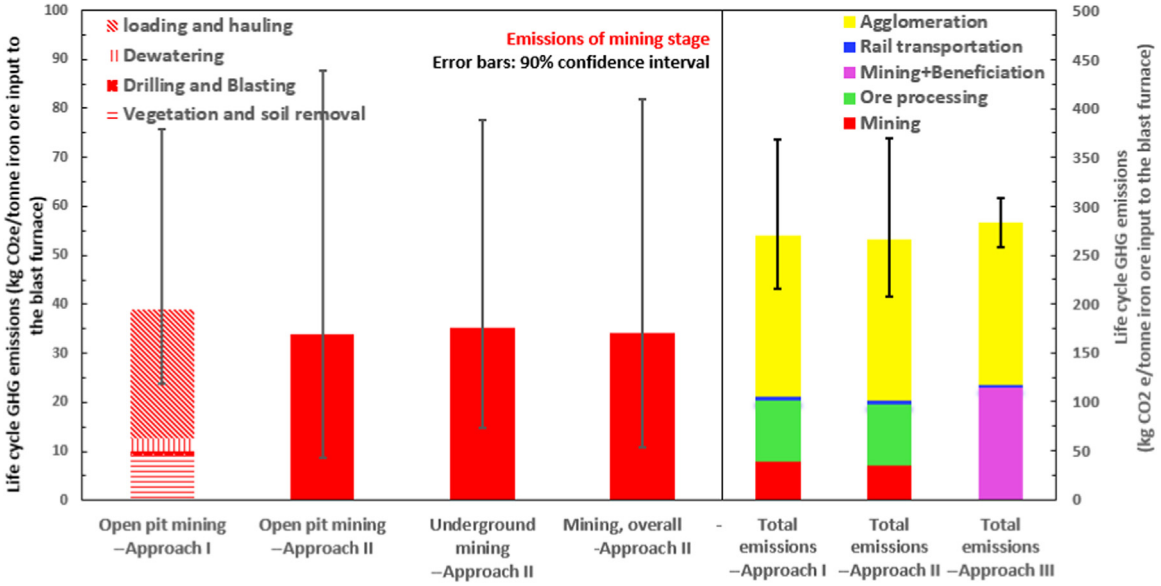

Fig. 2. GHG emissions for the iron ore mine phase and life cycle emissions for Chinese iron ore mining for a 1 kg of iron ore to the blast furnace. The error bars represent the 90% confidence interval from the Monte Carlo simulation. Three approaches were used to estimate associated emissions of mining stage: Approach I is a bottom up assessment; Approach II used mining plants data reported by Department of Metallurgy of China; Approach III used statistical energy data of iron mining and processing sector, LCA results using this approach aggregates emissions for mining and ore processing stages.

to 11% in 2015. The higher market price of pellets compared with sinters is claimed to be the primary reason for the growth stagnation (Manxing, 2001). Establishing financial aids for pelletizing (e.g. subsidy and tax reduction) might be a viable way to promote the further development of pelletizing. A detailed economic analysis should be conducted before taking further actions.

The second largest source of GHG emissions is ore processing, where the iron content is increased to produce concentrated fines. Compared with the high-grade ore of other major producing areas, such as Australia or Brazil that have ores over 50% Fe content, 94% of Chinese crude ores are low grade, averaging around 27% Fe in 2012 (China Steel Yearbook, 2014).

High-grade ores (over 60% Fe content), require only simple processing while the low-grade ores require more complicated treatment processes and involve additional steps of milling, floatation/magnetic separation, concentration, filtration, and drying. This complexity comes at the cost of increased energy consumption in the form of electricity. As over 70% of Chinese grid electricity is sourced from coal and peat, the GHG emissions are high.

Increasing iron mining and high-grade ore depletion in China necessitate the use of lower grade ore in the future. By varying the value of iron ore grade in the original model used for estimating life-cycle GHG emissions (Approach II) and maintaining other parameters constant, the study further discusses the change of GHG emissions as the iron ore grade decreases. The analysis results are shown in Fig. 3.

According to Fig. 3, the relationship between iron ore grade and GHG emissions is non-linear. As the iron ore grade declines, the rate of increase in GHG emissions from mining accelerates. For example, when iron ore grade decreases from 40% to 35%, the average GHG emissions for mining increases by 12 kg CO_2e/tonne. In contrast, the same 5% iron ore grade decrease from 20% to 15% would lead to 52 kg CO_2e/tonne. Thus, China will face accelerating energy consumption and increased GHG emissions for every tonne of iron ore extracted and processed in the future. From 2006 to 2012, average iron ore grade dropped from 30% to 27% (China Steel Yearbook, 2014). If this trend continued, in 2020, the average iron ore grade could be 23%, and life-cycle mean GHG emissions would increase by 9%, from 2012 level of 285 kg CO_2e/tonne to 310 kg CO_2e/tonne.

From 2001 to 2013, the total iron ore demand in China increased

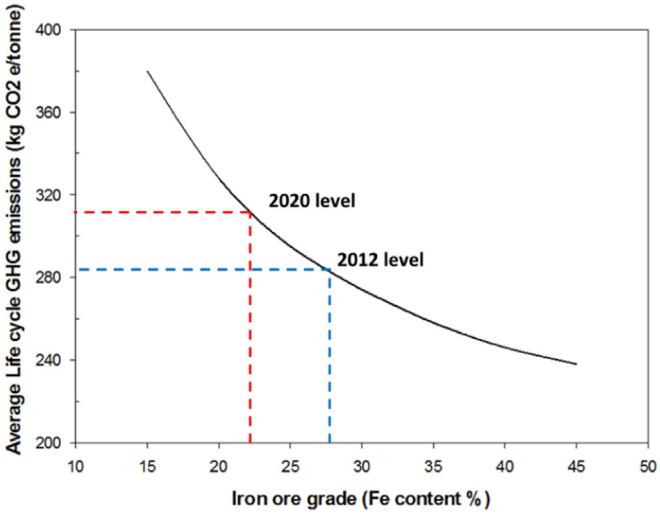

Fig. 3. Mean life-cycle GHG emissions per tonne of iron ore (total emissions–approach II, Fig. 2), as a function of iron ore grade.

with an average yearly growth rate of 15%. If the increase continues, the total GHG emissions for the iron ore mining/processing sector will increase three times that of the 2013 level by 2020, representative for 2.3% of the total projected GHG emissions for China in 2020 (Zhou et al., 2011), if the fraction of ore provided by the domestic supply remains unchanged.

4. Policy implications

It is possible that importing high-grade iron ores from other countries might be a viable GHG emissions reduction strategy for this important sector of the Chinese economy. For example, in Australia, iron ore has an Fe content of between 56% and 62% (Ferson, 1996), and most deposits are near the surface. Mining this ore would results in lower GHG emissions in the Chinese supply chain. However, detailed analysis of the GHG emissions associated with long distance shipping is needed, as shipping emissions could offset some of the emissions

savings due to the higher iron ore grade. Importing iron into China could lead to undesirable socioeconomic impacts making an assessment tradeoffs necessary. Potential impacts include decreased production in the Chinese mining sector leading to unemployment, as well as stability and security issues for the country's economic system.

Results shown here suggest that increasing the fraction of pelletized iron ore used in the blast furnaces can reduce overall GHG emissions. Using 100% pellets rather than the current sinter-pellet mix would reduce current life-cycle GHG emissions by 52%.

5. Conclusions

The present study analyzes the mean value and uncertain range of life-cycle GHG emissions associated with iron ore production in China. This study applies a multiple approaches using engineering calculations and multiple sources of sectoral energy data of different aggregation to determine the GHG emissions for mining and transporting iron to steel making firms in China. The results suggest that iron ore grade is the key parameter driving the LCA results, and that rapidly declining iron ore grade can accelerate increased GHG emissions in China. Importing high-grade iron ore from abroad, and increasing the fraction of pellets fed to the blast furnaces can reduce GHG emissions from iron ore production and use in China.

Acknowledgements

Funding for this research was provided by Carnegie Mellon College of Engineering (CIT) Dean's Fellowship, Carnegie Mellon Department of Engineering and Public Policy; the Fundação para a Ciência e a Tecnologia (Portuguese Foundation for Science and Technology) through the Carnegie Mellon Portugal Program; and Center for Climate and Energy Decision Making through a cooperative agreement between the National Science Foundation and Carnegie Mellon University (SES-0949710).

Appendix A. Supplementary material

Supplementary data associated with this article can be found in the online version at http://dx.doi.org/10.1016/j.resourpol.2018.03.015.

References

Akaike, H., 1974. A new look at the statistical model identification. Autom. Control IEEE Trans. 19 (6), 716–723.
Analysis of Diesel Use for Mine Haul and Transport Operations, 2010. Department of Resource, Energy and Tourism, Australian Gorernment.
Anshan Iron and Steel Group Mining Company Qidashan Mining Rights Assessment Report, 2013. Liaoning Huanyu Mining Consulting Ltd., Liaoning. ⟨http://www.mlr.gov.cn/kqsc/kqpg/pgbg/201409/P020140905367899539205.pdf⟩.
AusLCA Datasets, 2011. Australian Life Cycle Assessment Society. ⟨http://alcas.asn.au/AusLCI/index.php/Datasets⟩.
Benxi Iron & Steel (group) CO., LTD Website. ⟨http://www.bxsteel.com/bxsteel/homepage.html⟩.
Chang, S., 2010. Exploitation of resources and transformation of mining technology in Baiyunebo iron mine. Sci. Technol. Baotou Steel 6, 3.
Chen, W., Yin, X., Ma, D., 2014. A bottom-up analysis of China's iron and steel industrial energy consumption and CO2 emissions. Appl. Energy 136, 1174–1183.
China Steel Yearbook 2013, 2014. China Steel Development and Research Institute, Beijing.
China's Regional Grid Baseline Emission Factors 2010 for New Grid Connected Fossil Fuel Fired Power Plants Using A Less GHG Intensive Technology Projects, 2010. National Development and Reform Commission, Department of Climate Change, Beijing. ⟨http://cdm.ccchina.gov.cn/WebSite/CDM/UpFile/File2537.pdf⟩.
Domingues, A.F., Boson, P.H.G., Alípaz, S., 2013. Water Resource Management and The Mining Industry. National Water Agency, Brasília.
Emissions & Generation Resource Integrated Database. United States Environmental Protection Agency. ⟨https://www.epa.gov/energy/emissions-generation-resource-integrated-database-egrid⟩.
Fang, J., Guo, Z., Piao, S., Chen, A., 2007. Terrestrial vegetation carbon sinks in China, 1981–2000. Sci. China Ser. D: Earth Sci. 50 (9), 1341–1350.
Ferreira, H., Leite, M.G.P., Life Cycle, A., 2015. Assessment study of iron ore mining. J. Clean. Product. 108, 1081–1091.
Ferro Metallurgy and Mining Statistical Yearbook 2011, 2012, Department of Metallurgy, Chinese Government.
Ferson, S., 1996. What Monte Carlo methods cannot do. Hum. Ecol. Risk Assess. 2 (4), 990–1007.
Friedlingstein, P., Andrew, R.M., Rogelj, J., Peters, G.P., Canadell, J.G., Knutti, R., Luderer, G., Raupach, M.R., Schaeffer, M., Van Vuuren, D.P., 2014. Persistent growth of CO2 emissions and implications for reaching climate targets. Nat. Geosci. 7 (10), 709–715.
Haberl, H., Erb, K.H., Krausmann, F., Gaube, V., Bondeau, A., Plutzar, C., Gingrich, S., Lucht, W., Fischer-Kowalski, M., 2007. Quantifying and mapping the human appropriation of net primary production in earth's terrestrial ecosystems. Proc. Natl. Acad. Sci. USA 104 (31), 12942–12947.
Hasanbeigi, A., Morrow, W., Sathaye, J., Masanet, E., Xu, T., 2013. A bottom-up model to estimate the energy efficiency improvement and CO2 emission reduction potentials in the Chinese iron and steel industry. Energy 50, 315–325.
Imhoff, M.L., Bounoua, L., 2006. Exploring global patterns of net primary production carbon supply and demand using satellite observations and statistical data. J. Geophys. Res. 111.
Iosif, M., Hanrot, F., Ablitzer, D., 2008. Process integrated modelling for steelmaking life cycle inventory analysis. Environ. Impact Assess. Rev. 28 (7), 429–438.
IPCC 2007 as Climate change 2007: impacts, adaptation and vulnerability: contribution of Working Group II to the fourth assessment report of the Intergovernmental Panel on Climate Change. Intergovernmental Panel on Climate Change (IPCC): 2007.
Jones, G.M., Bosserman, B.E., Sanks, R.L., Tchobanoglous, G., 2006. Pumping Station Design. Gulf Professional Publishing, Burlington, Massachusetts, US.
Karali, N., Xu, T., Sathaye, J., 2014. Developing long-term strategies to reduce energy use and CO2 emissions—analysis of three mitigation scenarios for iron and steel production in China. Mitig. Adapt. Strateg. Global Change 1–21.
Kecojevic, V., Komljenovic, D., 2011. Impact of Bulldozer's engine load factor on fuel consumption, CO_2 emission and cost. Am. J. Environ. Sci. 7 (2), 125.
Kogel, J.E., 2006. Industrial minerals & rocks: commodities, markets, and uses. SME.
Kumar, S., Srinivasan, T.M., 2010. Sintering and Pelletisation of Indian Iron Ores. Mineral Enterprise Limited, Bangalore.
Li, G., Nie, Z., Zhou, H., Di, X., Liu, Y., Zuo, T., 2002. An accumulative model for the comparative life cycle assessment case study: iron and steel process. Int. J. Life Cycle Assess. 7 (4), 225–229.
Li, L., Lei, Y., Pan, D., 2016. Study of CO2 emissions in China's iron and steel industry based on economic input–output life cycle assessment. Nat. Hazards 81 (2), 957–970.
Life Cycle Inventory Database, 2014. National Renewable Energy Laboratory. ⟨https://www.lcacommons.gov/nrel/search⟩.
Lixue, J., Xunmin, O., Linwei, M., Zheng, L., Weidou, N., 2013. Life-cycle GHG emission factors of final energy in China. Energy Procedia 37, 2848–2855.
Manxing, X., 2001. Improvement and development of blast furnace burden design in China. Sinter. Pelletizing 2, 001.
Mines Overview. Baotou Steel Group Barun Mining Co., Ltd. ⟨http://www.byebbr.com/services.html⟩.
New Millennium Capital Corp, 2010. A Technical Report on the Feasibility study of the Direct Shipping Iron Ore (DSO) Project. New Millennium Capital Corp : Montreal, Canada.
Norgate, T., Haque, N., 2010. Energy and greenhouse gas impacts of mining and mineral processing operations. J. Clean. Prod. 18 (3), 266–274.
Pero, L., 2011. The Downer Energy and Emissions Measure. In: Energy Efficiency Opportunities Workshop 2011.
Pidwirny, M., Primary Productivity Table. ⟨http://www.world-builders.org/lessons/less/biomes/primaryP.html⟩.
Robusto, C., 1957. The cosine-haversine formula. Am. Math. Mon. 38–40.
Ruesch, A., Gibbs, H.K., 2008. New IPCC Tier-1 global biomass carbon map for the year 2000. Carbon Dioxide Inf. Anal. Center. ⟨http://cdiac.ornl.gov/epubs/ndp/global_carbon/carbon_documentation.html⟩.
Scott Matthews, H., Hendrickson, Chris T., Matthews, Deanna, 2014. Life Cycle Assessment: Quantitative Approaches for Decisions that Matter. Publicly available via ⟨http://www.lcatextbook.com/⟩.
Shen, L., Cheng, S., Gunson, A.J., Wan, H., 2005. Urbanization, sustainability and the utilization of energy and mineral resources in China. Cities 22 (4), 287–302.
SimaPro LCA Software, 2008. Product Ecology Consultants: Amersfoort, Netherlands. ⟨http://www.pre.nl/⟩.
Stewart, M., 2001. Report of Life Cycle Assessment Workshop: The Application of LCA to Mining, Minerals and Metals. International Institute for Environment and Development, London, UK. ⟨http://pubs.iied.org/pdfs/G00942.pdf⟩.
Tannant, D.D., Regensburg, B., 2001. Guidelines for Mine Haul Road Design. School of Mining and Petroleum Engineering, Department of Civil and Environmental Engineering, University of Alberta.
Teale, R., 1965. The concept of specific energy in rock drilling. Int. J. Rock Mech. Min. Sci. Geom. Abstr. 57–73.
The Chinese Energy Statistics Year Book, 2012. Energy Statistics Division of National Bureau of Statistics. China Statistics Press, Beijing.
U.S. Geological Survey website. ⟨http://www.usgs.gov/⟩.
Venkatesh, A., Jaramillo, P., Griffin, W.M., Matthews, H.S., 2010. Uncertainty analysis of life cycle greenhouse gas emissions from petroleum-based fuels and impacts on low carbon fuel policies. Environ. Sci. Technol. 45 (1), 125–131.
Volk, M., 2013. Pump Characteristics and Applications. CRC Press, Boca Raton, Florida, US.
World Steel Life Cycle Inventory (2000) Methodology Report, 2000. International Iron and Steel Institute, Brussels.
Yu, D., Shi, X., Wang, H., Sun, W., Chen, J., Liu, Q., Zhao, Y., 2007. Regional patterns of soil organic carbon stocks in China. J. Environ. Manag. 85 (3), 680–689.
Zhou, N., Fridley, D., McNeil, M., Zheng, N., Ke, J., Levine, M., 2011. China's Energy and Carbon Emissions Outlook to 2050. Ernest Orlando Lawrence Berkeley National Laboratory, Berkeley, CA (US).